Int J Adv Manuf Technol (2018) 95:2495–2508
DOI 10.1007/s00170-017-1091-6

ORIGINAL ARTICLE

Experimental and simulation research on micro-milling temperature and cutting deformation of heat-resistance stainless steel

Zhenxin Peng[1] · Jiao Li[2] · Pei Yan[2] · Shoufeng Gao[1] · Chenhong Zhang[1] · Xibin Wang[2]

Received: 12 April 2017 / Accepted: 12 September 2017 / Published online: 24 November 2017

Abstract n view of the influence of cutting heat and cutting force on the machining precision of micro-machining, this paper carries out micro-milling temperature measurements and deformation measurement tests based on the theoretical model of temperature field distribution of workpiece and the simulation model of workpiece deformation, providing technical basis for the high-precision machining of precision micro-parts. A theoretical model for the description of the increase in the cutting temperature of the workpiece is established prior to using an inverse evaluation method for solving the heat source intensity iteratively. During the finite element analysis of the distribution of the temperature field and heat distortion, the process of the heat transfer is simplified as a process of applying a series surface heat source to workpiece. Besides, this paper carried on a series of micro-milling experiments, used a fast-response thermocouple which has a property of self-renewal for the measurement of the change of the workpiece temperature, the response time of the applied thermocouple is within the magnitude of micro-second, and then, a high-frequency amplifier and an electric potential acquisition equipment were used to gain the transient temperature in the cutting area; meanwhile, a dynamometer is applied to measure the three-directional forces, and finally, the workpiece deformation would be measured by the Keyence microscope. Through the comparison of the simulated temperature and deformation with the experimental results, the simulation model showed considerable reliability.

Keywords Micro-milling · Machining precision · Heat source method · Workpiece deformation · Prediction model

✉ Jiao Li
JiaoLi@bit.edu.cn

[1] School of Mechanical Engineering, Beijing Institute of Technology, Beijing, China

[2] Key Laboratory of Fundamental Science for Advanced Machining, Beijing Institute of Technology, Beijing, China

Nomenclature

θ	Temperature rise function
q_m	Heat source intensity
k	Thermal conductivity
l	Heat source width
a	Temperature coefficient
v_f	Heat source velocity
K_0	Zero order second modified Bessel function
x	X coordinates of any point
y	Y coordinates of any point
z	Z coordinates of any point
x_q	X point coordinates on the heat source
y_q	Y point coordinates on the heat source
z_q	Z point coordinates on the heat source
X	X coordinates of a point on the workpiece
Y	Y coordinates of a point on the workpiece
Z	Z coordinates of a point on the workpiece
t	Milling time
D	Distance from the temperature measuring point to the heat source
θ_s	The temperature model of the shear surface heat source
θ_s	The temperature model of the mirror heat source
q_s	Shear surface heat sources
q_s'	Mirror heat source
ε	The coangle of the shear angle
I	The number of measuring points
T_{im}	The i point's predicted temperature of time t_m
Y_{im}	The i point's measured temperature of time t_m

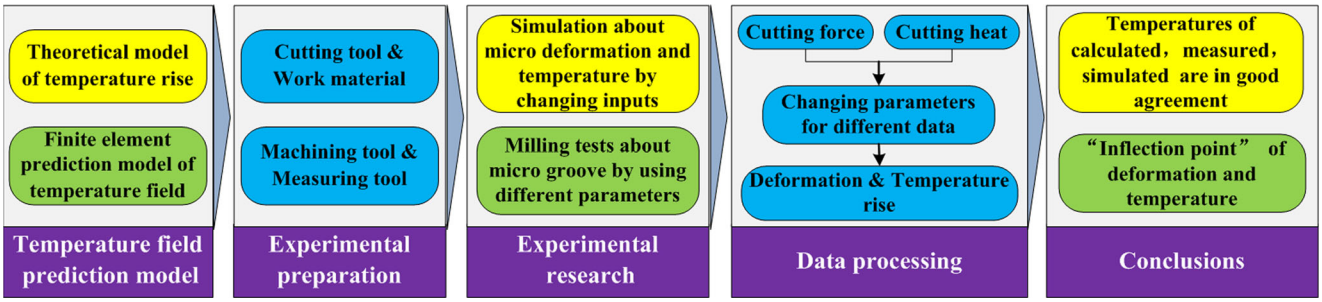

Fig. 1 The general structure scheme

ϕ_{im} Sensitivity coefficient
n Rotation speed of the spindle
f Feed speed
a_p Axial cutting depth
v_c Cutting speed
N Number of tests
d Slot width

1 Introduction

Currently, an increasing number of micro-parts and micro-components are being widely used in various fields including biomedical engineering, instrument manufacturing, aerospace engineering, and micro-robotics. The micro-miniaturization of products has become a significant developing direction of modern manufacturing industry and moreover micro-cutting technology has become a research hotspot [1–3]. In order to reveal the difference in mechanism between micro- and macro-cutting, many scholars have conducted studies on the micro-cutting [4–8].

Cutting heat and cutting force directly affect the wear and service life of the tool, thereby affecting the machining accuracy and surface quality of the workpiece. The error caused by thermal deformation has reached 50% of the total manufacturing error of modern machine tools, so it is significant to study on the generation and variation of cutting heat [9, 10]. In view of the cutting heat in the milling process, scholars have carried out a series of research. Li et al. [11] aimed at shear surface deformation heat source and tool flank wear heat source established the temperature variation model of the workpiece by mathematical method. According to Grzesik et al. [12], that the friction of tool-chip contact area is the most important factor of cutting temperature. Jiang et al. [13] studied on the changes of tool and workpiece temperature in 1045 steel intermittent

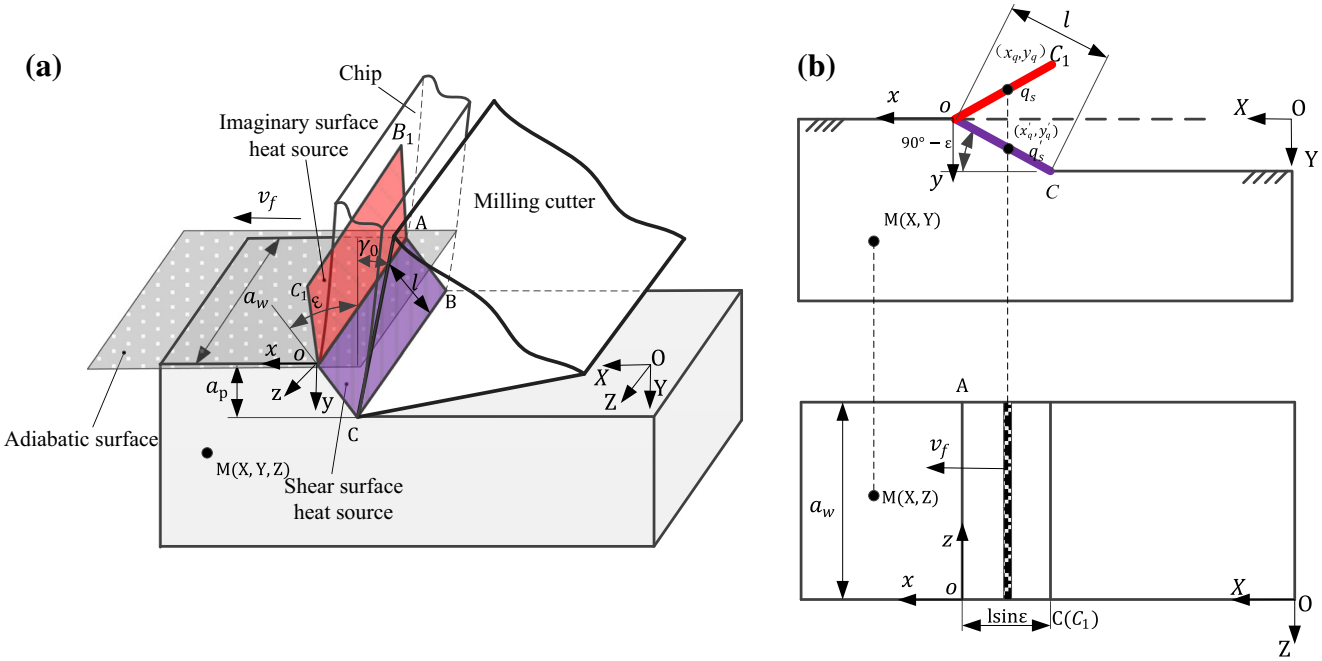

Fig. 2 Schematic diagram of shear plane heat source

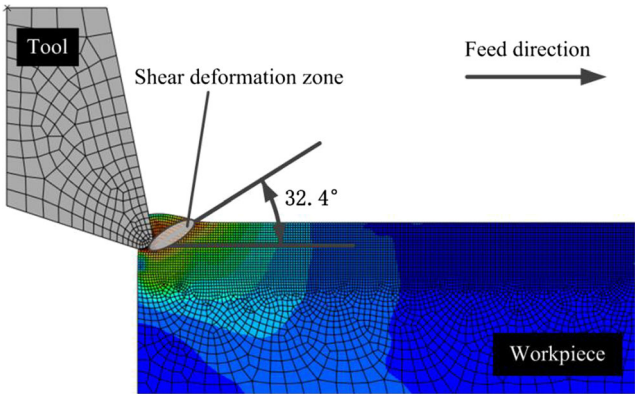

Fig. 3 The prediction model of shear angle

milling, thereby basing on heat source method and inverse method analyzed the effect of milling depth and tool-chip contact length on temperature variation. Carvalho et al. [14] analyzed the influence of cutting parameters on cutting edge temperature field by applying the inverse heat conduction method. Rai et al. [15] made use of the ANSYS sequential thermal-mechanical coupling method to simulate the characteristics of cavity, groove, and ladder. Lazoglu et al. [16] simulated the temperature distribution of workpiece and cutter contact surface in the milling process. Yang et al. [17] obtained the temperature variation curve of the milling process through finite element simulation; furthermore, during the milling process, the temperature of titanium alloy was measured by means of semi-artificial thermocouple. Hsu et al. [18] studied the properties of machining MAR-M247 nickel-based superalloy combined ultrasonic vibration with high-temperature-aided cutting. The Taguchi experimental design was adopted to identify the influence of machining parameters on the machining characteristics. Aimed at the cutting temperature Salomon curve which appeared in high-speed milling, Zhang et al. [19] revealed the effect of cutting speed on the cutting temperature by combining the

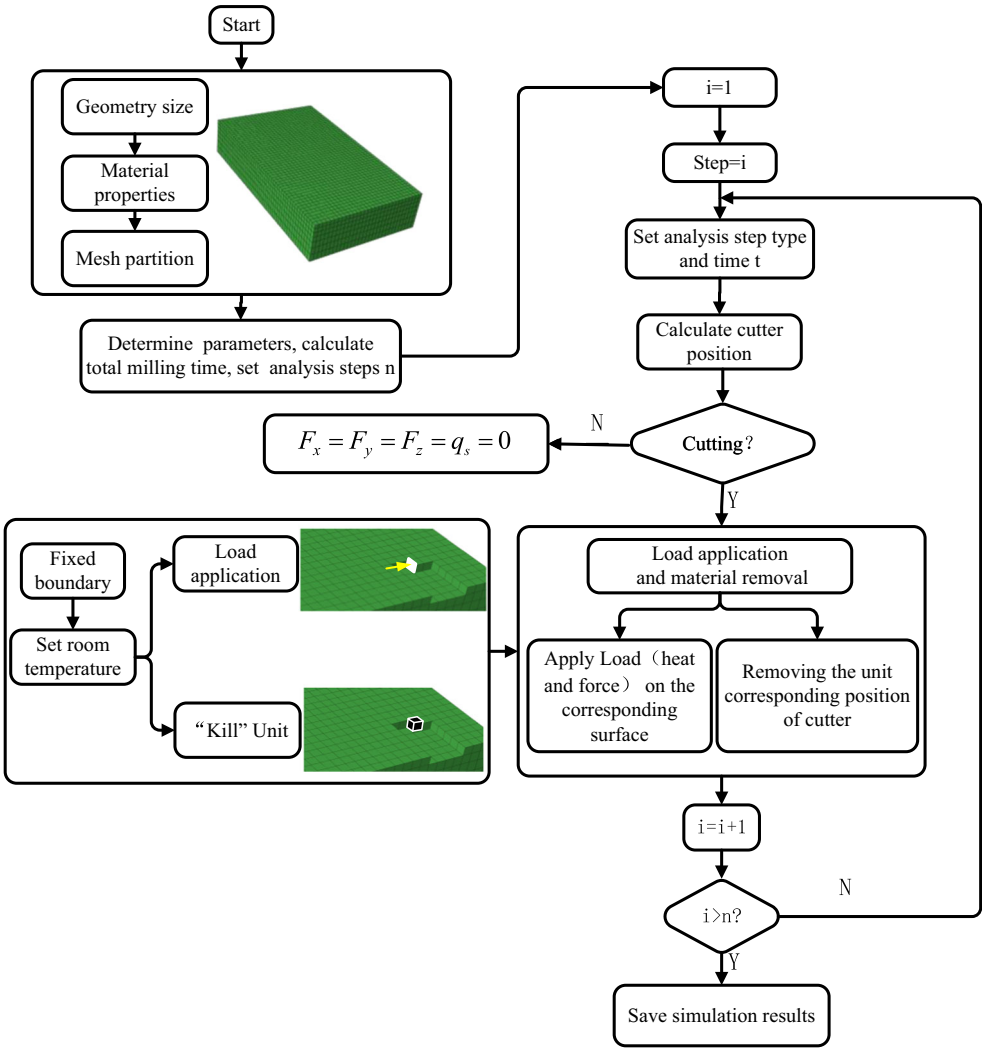

Fig. 4 Flow chart of simulation analysis

Table 1 Simulation material parameters

Density (kg/m^3)	Elastic modulus (GPa)	Poisson ratio	Thermal conductivity (W/(m °C))	Specific heat (J/(kg °C))	Average coefficient of thermal expansion (10^{-6} m/°C)
7760	196	0.29	11.9	472	18.8

analytical method, finite element simulation, and experimental measurement. Luo et al. [20] established the finite element model of thermo-mechanical coupling, by that, explored the effect of cutting parameters on the cutting temperature field distribution. Tang et al. [21] constructed the instantaneous milling force model, the milling thermal model, and the material constitutive model; these models succeeded to predict the deformation of the workpiece under the milling force and milling heat. Liu et al. [22] measured the temperature of the milling cutter blade in the milling process by using embedded thermocouple, thereby established the corresponding theoretical calculation model and the finite element simulation model. Richardson et al. [23] measured the instantaneous temperature of circumferential milling utilizing a fast-response semi-artificial thermocouple. Kaminise et al. [24] studied on the influence of cutter holder on turning temperature by using a semi-artificial thermocouple. In order to verify the validity of the theoretical model of the temperature field and observe trend that the workpiece temperature varies with the cutting speed, Zhang et al. [19] designed several high-speed milling experiments, measured the temperature of a certain point on the machined surface using a thermocouple, and finally obtained the heat source intensity through the inverse method. Chen et al. [25] carried out simulation modeling research and experiments about the temperature change of micro-cutting tool and the workpiece next turned out that the error between simulation modeling and experiment was within the ideal range. It could be concluded from Rahman et al. [26–29] that cutting fluids posed serious health and environmental hazards and applying cutting fluid had little effect on the heat of the plastic deformation slip shear zone during cutting process.

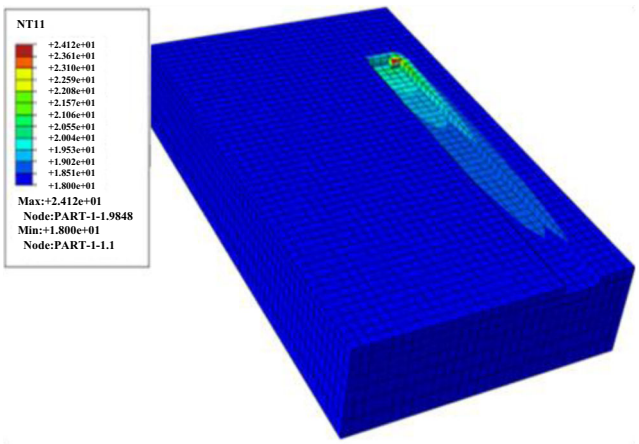

Fig. 5 Temperature field nephogram

The aforementioned studies have used different methods to study the effect of milling heat and milling force on the workpiece deformation, but most of them are conducted under the conventional cutting conditions. Based on previous studies, this paper carried out a series of innovative research on micro-milling. Organization for the remainder of this paper is as follows: firstly, a theoretical model of the temperature field is established, based on which the predictions and simulations of the micro-milling temperature and deformation are discussed in Section 2. In Section 3, a number of cutting experiments with altering milling parameters (spindle speed, feed rate, cutting depth) are carried out by using end milling cutters with a diameter of 2 mm; thereafter, the experimental results are analyzed and discussed in Section 4. Finally, conclusions drawn from this research are given in Section 5. The general structure scheme of this article is presented as shown in (Fig. 1).

2 Temperature field prediction model

2.1 Theoretical model of temperature rise

During the milling process, the cutting heat is mainly located in three regions: the plastic deformation slip shear zone, the zone between tool rake face and chip, and the zone of machined surface affected by the friction and extrusion of the flank. The first deformation zone is the main source of cutting heat, because it produces a large amount of shear deformation energy. The second deformation zone has a negligible influence on the workpiece temperature field, because the heat mainly transfers into the chip. In addition, the friction heat between tool flank and workpiece caused by micro-cutting can also be ignored.

For a heat source with a certain shape, size, and under a definite dynamic situation, the heat source method could solve the problem of understanding the effect of heat source on heat-transfer medium more directly. During the milling process, the temperature model of a planar strip heat source moving in a semi-infinite solid could be given by Hou and Jaeger [30]:

$$\theta = \frac{q_m}{\pi k}\int_0^l e^{\frac{(x-x_q)v_f}{2a}} \cdot K_0\left[\frac{v_f}{2a}D\right] d_{x_q}$$

In the formula, D is the distance from the temperature measuring point to the heat source, $D = \sqrt{(x-x_q)^2 + (y-y_q)^2}$, and K_0 is zero order second modified Bessel function.

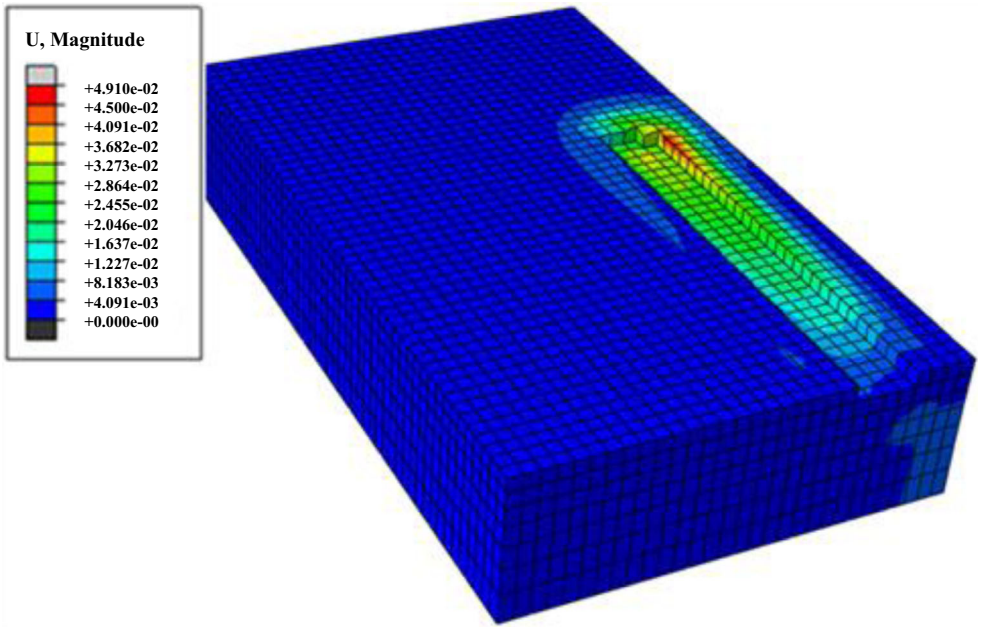

Fig. 6 Deformation field nephogram

The coordinate system is shown in Fig. 2. A boundary point of unfinished workpiece as the origin of static coordinate system, the intersection between the shear surface and the surface to be machined on the side of the workpiece as the origin of coordinate system, feed direction as positive direction of X axis, milling depth direction as direction of Y axis, milling width direction as direction of Z axis. The Y and Z coordinates are the same between the two coordinate systems, the relation of X coordinate system is $X = x - v_f t$ and t is milling time.

In the actual milling process, during which no coolant is applied, it can be assumed the workpiece to be adiabatic since the convection heat transfer coefficient between the workpiece and the surrounding air is very small. Aimed at the machined, the front and the back surface, using the method of mirror heat source, the temperature model of the shear surface heat source and its mirror heat source can be obtained:

$$\theta_s = \frac{q_s}{\pi k}\int_{-1\sin\varepsilon}^{0} e^{\frac{\left(X-v_f t-x_q\right)v_f}{2a}} K_0\left[\frac{v_f}{2a}\sqrt{\left(X-v_f t-x_q\right)^2+\left(Y+\frac{x_q}{\tan\varepsilon}\right)^2}\right] d_{x_q}$$

$$\theta_s' = \frac{q_s'}{\pi k}\int_{-1\sin\varepsilon}^{0} e^{\frac{\left(X-v_f t-x_q'\right)v_f}{2a}} K_0\left[\frac{v_f}{2a}\sqrt{\left(X-v_f t-x_q'\right)^2+\left(Y-\frac{x_q'}{\tan\varepsilon}\right)^2}\right] d_{x_q'}$$

In the formula, ε is the complement angle of the shear angle which can be predicted accurately by applying the finite element simulation model (as shown in Fig. 3).

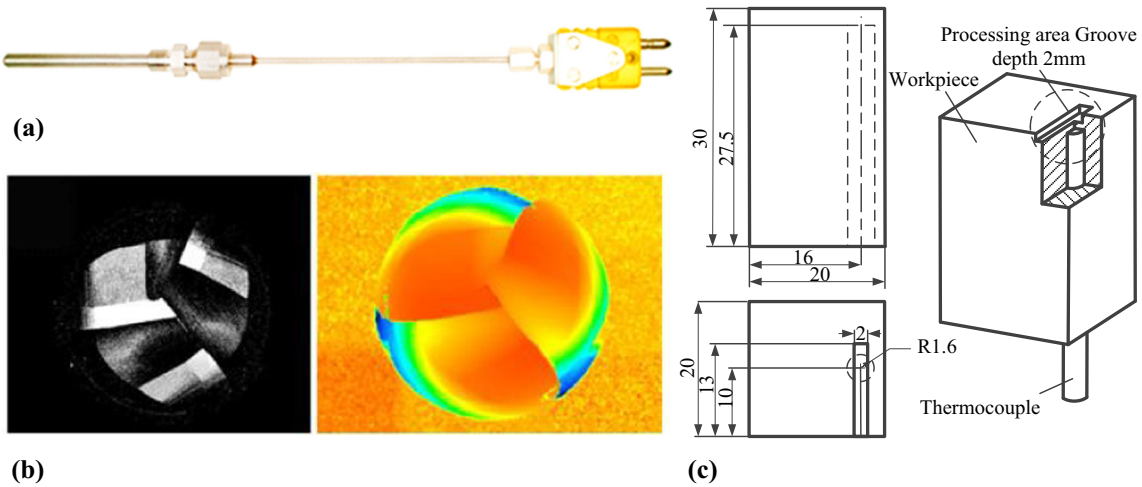

Fig. 7 **a** Thermocouple. **b** End milling cutter. **c** Schematic diagram of workpiece

Table 2 Thermocouple parameters

Model	Probe size	Measuring range	Thermometric accuracy	Response time
E12-3-K-U	$\phi 3.175 \times 101.6$	0–1350 °C	0.25%	20 μs

Based on the inverse method [31], the heat source intensity (q_m) can be easily and accurately calculated. First, using the least square method, the relation about heat source intensity and temperature (T_m) is

$$f(q_m) = \sum_{i=1}^{I} (Y_{im} - T_{im})^2$$

In the formula, I is the number of measuring points, T_{im} is the predicted temperature of point i at time t_m, and Y_{im} is the measured temperature of point i at time t_m. Then, finding derivatives of the aforementioned formula, q_m could be obtained:

$$q_m = \frac{\sum_{i=1}^{I} \left(Y_{im} - T_{im}\big|_{q_m=0}\right)\phi_{im}}{\sum_{i=1}^{I} \phi_{im}^2}$$

In the formula, ϕ_{im} is the sensitivity coefficient and can be obtained:

$$T_{im} = T_{im}\big|_{q_m=0} + \phi_{im} q_m$$

2.2 Finite element prediction model of temperature field

Based on the theoretical model of temperature rise, the finite element model of temperature field and thermal deformation can be established using the finite element software ABAQUS. As is well known, cutting force and cutting heat interrelate during the milling: first, shear slip and plastic deformation would occur in cutting area due to the cutting force; next, in the cutting area, temperature rises in result of which the work of the plastic deformation and the friction turn into heat, thereby causing thermal strain and then softening the material; furthermore, force cutting the softened material would become smaller than before and causing work to be reduced, thus turning out less heat; finally, the material would be hard and more force would be need. In a word, there is a complex temperature field and stress field in the milling process, it is a typical thermal-mechanical coupling problem. The thermal-mechanical coupling model, established by ABAQUS, could predict and analyze the temperature field and the deformation field. The flow chart of the simulation analysis is shown in Fig. 4.

Table 3 Tool parameters

Tool material	Diameter	Number of cutting edges	Helix angle	Cutting edge radius
Cemented carbide	2 mm	3	45°	5.28 μm

Table 4 The chemical composition of 06Cr25Ni20

Chemical element	C	Si	Mn	P	S	Ni	Cr
Content/%	0.1	1.5	2.0	0.045	0.015	19.0–22.0	24.0–26.0

The material parameters in simulation analysis is shown in Table 1, and eight-node hexahedron thermal coupling reducing integral unit (C3D8RT) has been chosen for the model unit. Some of the advantages the unit include the following: the solving of the thermal-mechanical coupling problem; the freedom of displacement and temperature; it could get better calculation accuracy compared to tetrahedron element in a complex stress environment. In an actual installation, the workpiece is fixed on the special fixture, and the fixture is connected to the Kistler dynamometer by screws, so six degrees of freedom constraints are exerted at the bottom of the workpiece in the simulation analysis. In addition, the temperature field is set to be adiabatic because of dry cutting. In order to simplify the model and improve the reliability of the predicted value, the maximum surface heat source is applied to the finite element model and kept constant.

2.3 Simulation result

As shown in Fig. 5, during the simulation process, the temperature change is mainly concentrated in the workpiece processing area (adjacent to the trajectory region of tool rotation). When milling, the heat generated and transferred into the workpiece will result in a rapid rise of temperature. The temperature of workpiece will rise continuously during the whole milling process. When the milling finishes, the heat source load and force load are removed, the temperature of the workpiece gradually decreases to the initial ambient temperature.

As shown in Fig. 6, during the simulation process, the workpiece deformation, same as the temperature change, is mainly concentrated in the processing area. During milling, shear slip and plastic deformation would occur on the workpiece under thermal-mechanical coupling and the deformation continuously changes during the whole milling process. When the milling finishes, elastic plastic recovery, finally stable within a certain range, would occur on the workpiece. According to the finite element simulation, given specific parameters (Spindle speed 8000 r/min, feed rate 20 mm/min, cutting depth 0.2 mm), it can be predicted that the maximum deformation value of groove width is 49.095 μm.

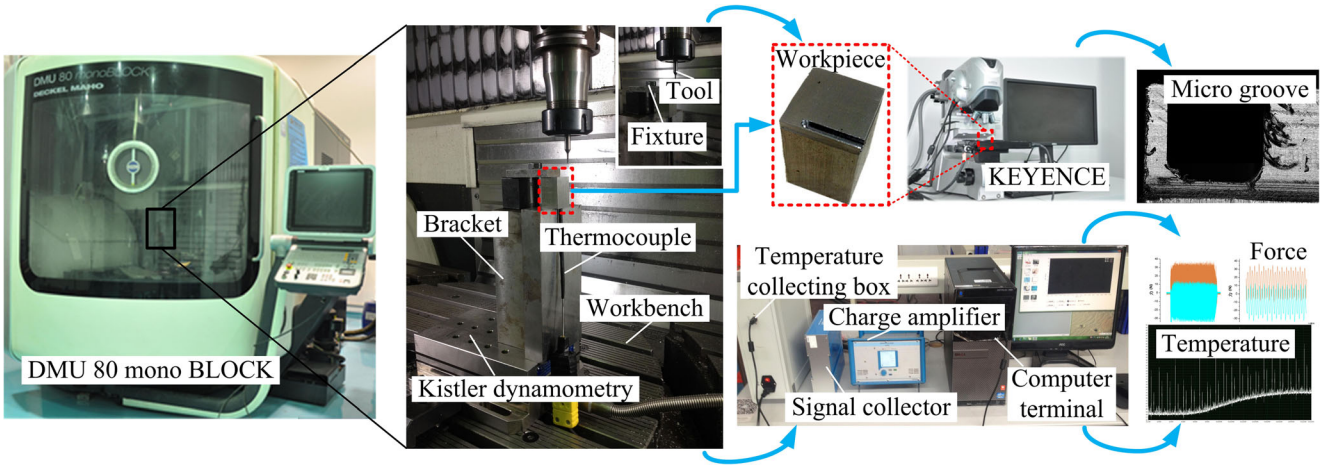

Fig. 8 Experimental platform and measurement platform

3 Micro-milling experiments

3.1 Thermocouple and cutting tool

In order to obtain a more accurate temperature of the machining region, a special fast-response thermocouple (NANMACTM, type E12), shown in Fig. 7a, is used in the experiments. The thermocouple has two distinct advantages: the probe of the thermocouple can be made of any machinable materials for matching the thermal characteristics of the workpiece and its response speed is higher than that of a general thermocouple, which could measure temperature variation, from 20 to 245 °C, in 8 μs.

Carbide cutting tools are widely used in the metal cutting of high-hardness materials in a large temperature range, in the experiments, as shown in Fig. 7b, the diameter of the tool is 2. The parameters of the thermocouple and the tool are shown in Tables 2 and 3.

3.2 Work material

The workpiece material chosen for this study is a heat-resistant stainless steel 06Cr25Ni20, a kind of austenitic stainless steel which has a good oxidation resistance and corrosion resistance. Moreover, high content of chromium and nickel gives it high creep strength and a good resistance to high temperature. It is commonly used in petroleum, electronics, chemical, pharmaceutical, textile, aerospace, and other fields. Figure 7c shows the specific size and shape of the workpiece, with the objective of accurately measuring the temperature, Table 4 lists the chemical composition of this material.

Table 5 Experimental conditions of milling tests with changing parameters

No.	n (r/min)	f (mm/min)	a_p (mm)	v_c (m/s)
1	5000	20	0.2	0.52
2	8000	20	0.2	0.84
3	10,000	20	0.2	1.05
4	12,000	20	0.2	1.26
5	10,000	15	0.2	1.05
6	10,000	20	0.2	1.05
7	10,000	25	0.2	1.05
8	10,000	30	0.2	1.05

3.3 Experimental set-up and design

Milling experiments are conducted in DMU 80 mono BLOCK milling center; during the cutting tests, dry cutting operation has been adopted. Because other factors have less influence on the results in dry cutting which is very suitable for the research of cutting force or cutting heat, the workpiece is fixed indirectly on a Kistler 9257B type three-component piezoelectric dynamometer, with the purpose of realizing real-time record of cutting force during the cutting. The cutting heat is measured by the thermocouple for obtaining the instantaneous temperature of cutting area. The configuration of the experimental set-up in machine tool is shown in Fig. 8.

In order to reduce the influence of tool wear on the cutting force and cutting heat, for each experiment, a separate tool was used. Since the effect of spindle speed and feed rate on cutting force and cutting heat is higher than that of cutting depth, the material removal rate needs to be precisely controlled; the experimental designs are shown in Table 5 (cutting depth is 0.2 mm). The effect of thermal-mechanical coupling on the deformation of workpiece is studied by two groups of single-factor experiments: group 1 is test nos. 1 to 4 about variable spindle speed with the same material removal rate and group 2 is test nos. 5 to 8 about variable feed rate with the different material removal rate.

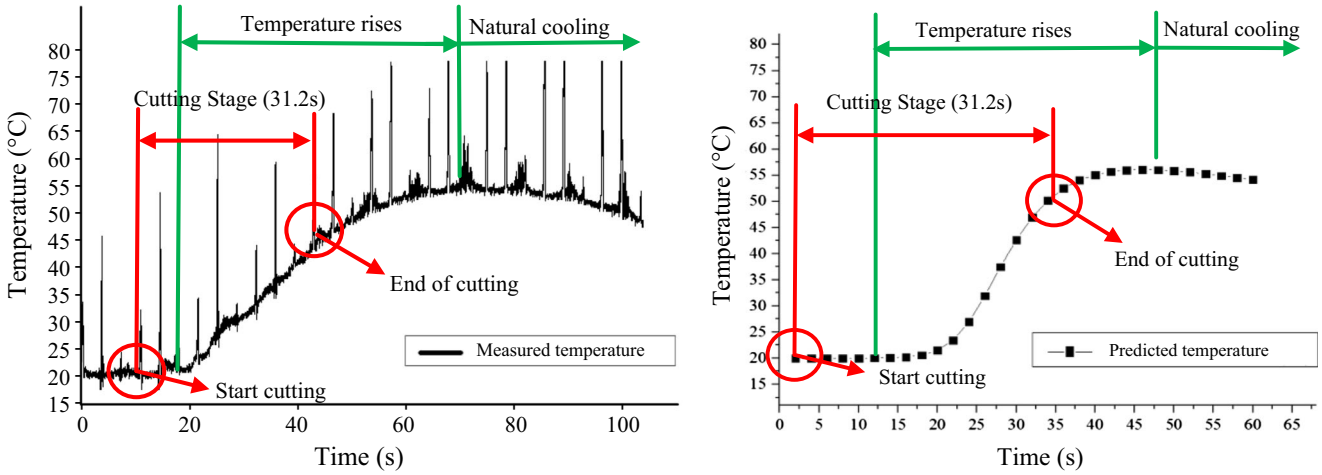

Fig. 9 Response table of workpiece temperature rise (n = 10,000 r/min; f = 25 mm/min; a_p = 0.2 mm) (**a**) Measured temperature, (**b**) Predicted temperature

3.4 Micro-milling workpiece temperature measurement

The instantaneous temperature (test no. 7) can be measured and predicted as shown in Fig. 9. With the intention of collecting an integral set of information, the temperature is measured before the tool starts cutting. As shown in Fig. 9a, in the actual cutting, the ambient temperature is about 20 °C. After 10 s, milling groove starts and workpiece temperature continues to rise, until the maximum temperature increases (57 °C) in 72 s. Finally, the workpiece would naturally cool in the air after the tool finishes cutting. In theory, the time required to mill the groove is 31.2 s, but it takes 54 s for the workpiece to increase temperature from the room temperature up to the maximum temperature. This could be reasoned that in an environment with a temperature range between 20 and 100 °C, the workpiece material is a heat-resistant stainless steel whose thermal conductivity is only 12 W/(m °C), less than 1/10 compared to 7075 aluminum alloy, causing the workpiece temperature rise to need more time than the milling process. In addition, the performance of the temperature measurement system also has a certain impact on the experimental results. Additionally, the temperature is lower than considered; it can be concluded that heat produced is lower in micro-cutting, and most of the heat is directly transferred into the air; furthermore, the thermocouple is relatively far away from the workpiece surface. In addition, the temperatures of measured and predicted instantaneous are in good agreement (variation trend and maximum value) as shown in Fig. 9a, b.

In Fig. 9a, most of the temperature data points are concentrated around the curve, but there still are some points far from the curve. The workpiece temperature does not suddenly become higher but when the temperature signal is converted into an analog signal of the thermal potential, this signal is often doped with other interfering signals; in other words, the noise filtering capacity of acquisition device is limited.

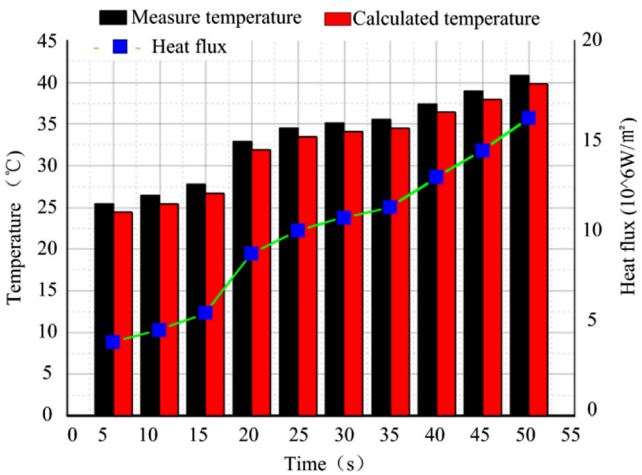

Fig. 10 Numerical results of heat flux

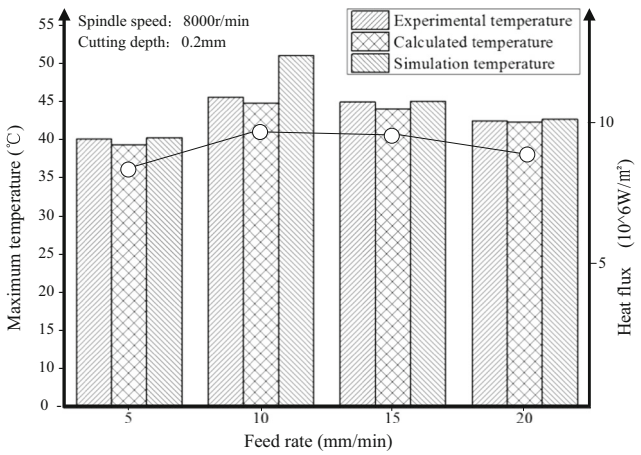

Fig. 11 Simulation-experimental-calculation temperature

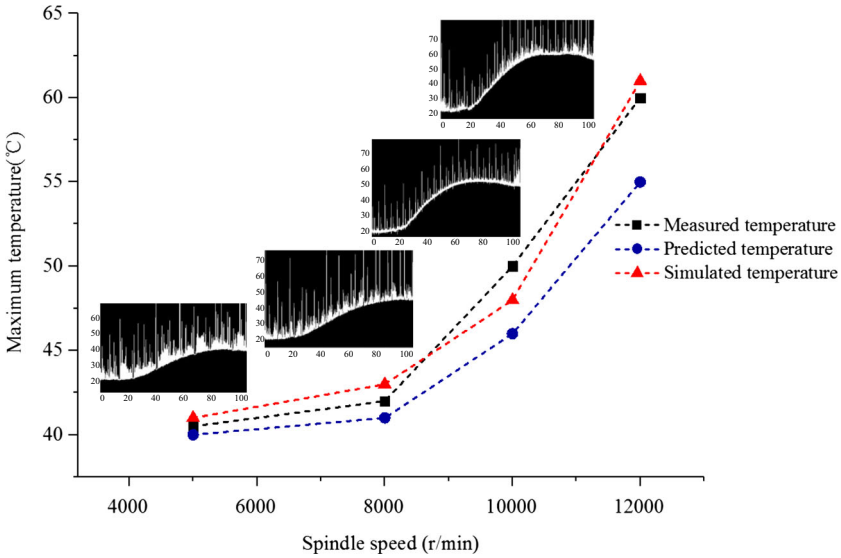

Fig. 12 The cutting temperature change of workpiece under different spindle speed

4 Experimental results and analysis

4.1 Analysis of temperature field prediction model

It is convenient to establish the instantaneous temperature incremental model by using the method of moving heat source, and the numerical calculation based on MATLAB programming simplifies the calculation process. In comparison to the instantaneous temperature rise curve of the workpiece, at n = 10,000 r/min and f = 25 mm/min, the temperature and surface heat source intensity values are obtained through the numerical calculation, which are shown in Fig. 10. As it can be seen, the calculated temperature and the measured temperature are in good agreement proving the correctness of this method.

The comparison of the measured and the calculated maximum temperature of the workpiece at different feed rates (at n = 8000 r/min) are shown in Fig. 11. As it can be seen, the measured cutting temperature is very low. It is because the stainless steel 06Cr25Ni20 is difficult to machine, the feed rate is adjusted to a very small value to protect the cutting tool. And the micro-cutting parameters are also very small, so the removal of material is very small, resulting in little cutting heat. The measurement of the cutting temperature is also affected by a series of factors such as the high thermal conductivity of the

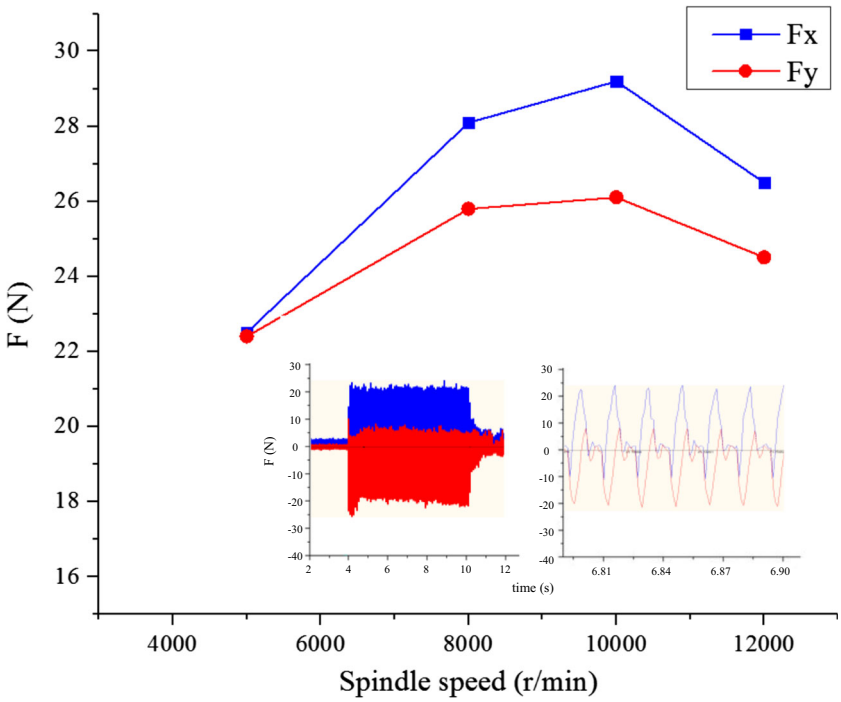

Fig. 13 The cutting temperature change of workpiece under different feed rate

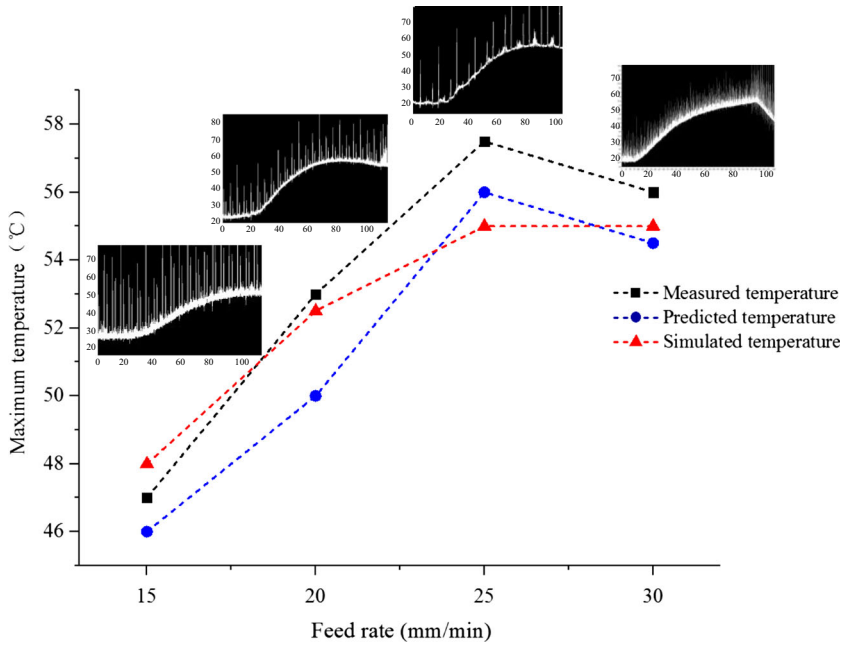

Fig. 14 The cutting force under different spindle speed

workpiece material and the distance between the thermocouple and the processing area. The measured temperature is used to calculate the sensitivity coefficient of the model. The calculated temperature, the measured temperature, and the simulated temperatures are in good agreement.

The cutting temperature increases at the beginning and decreases in the end with the increasing feed rate. It is because at the beginning, the cutting forces increases with the increasing feed rate, and in the end, the cutting time decreases as the feed rate increases.

4.2 Influence of cutting parameters on workpiece temperature

In order to study the influence of spindle speed on the cutting temperature, several experiments are carried out (test nos. 1 to

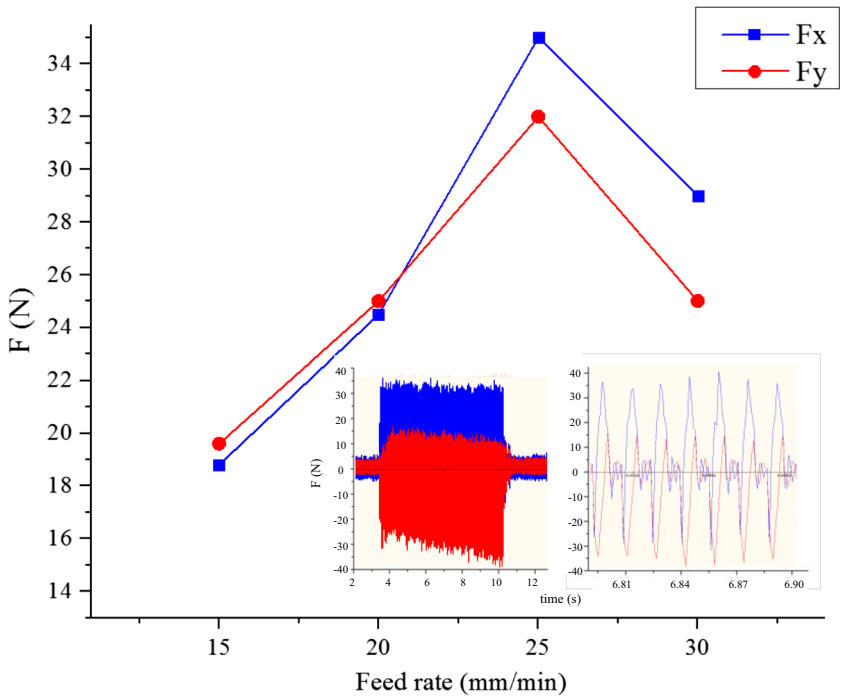

Fig. 15 The cutting force under different feed rate

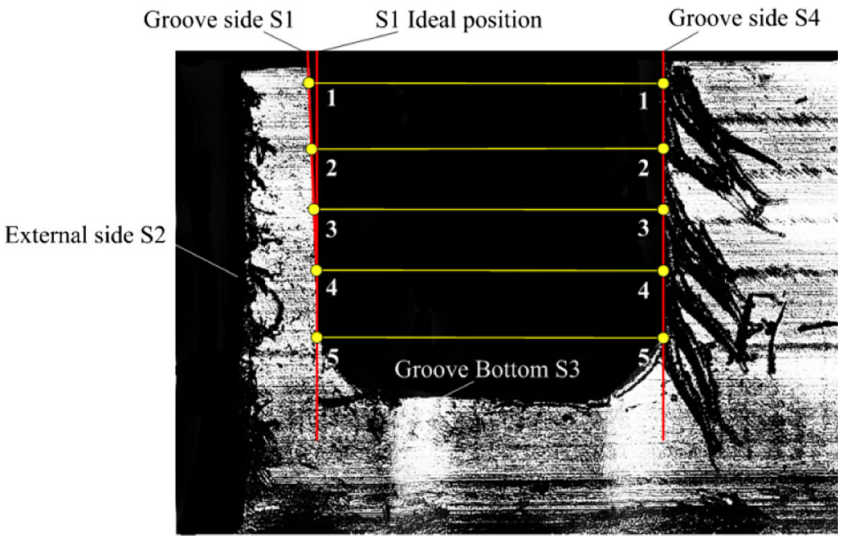

Fig. 16 Schematic diagram of the workpiece deformation

4). The layer to be removed is 2 mm and the total cutting time (four experiments) is about 20 min. The approximate temperature-rising curve is obtained by fitting, and the temperature of the workpiece is represented by the maximum temperature in the effective cutting time corresponding to the cutting parameters. The measured, the calculated, and the predicted cutting temperatures of the workpiece are shown in Fig. 12. As it can be seen, the cutting temperature increases as the spindle speed increases, which is because when the chip flows along the rake face and the bottom of the chip and the rake face have a strong friction, generating a lot of heat, and the friction heat is generated at the bottom of the thin chip. An interception in the chips is taken as a unit to investigate, where the friction heat is generated and conducted from side to side when the chip flows through the rake face. If the cutting speed is too large, the friction heat generated too fast to be transmitted to the cutting chip and the tool, resulting in accumulation in the bottom of the chip. In addition, with the cutting speed increasing, the amount of metal removal increases proportionally to unit time, and the power consumption increases; as a result the cutting heat will increase. But with the cutting speed increasing, the specific cutting force and the specific cutting power are reduced as shown in Fig. 13, thus causing the cutting heat and cutting temperature not to increase proportionally to the cutting speed.

In order to study the influence of feed speed on the cutting temperature, several experiments are carried out (test nos. 5 to 8). Corresponding to the cutting parameters, the temperature of the workpiece is represented by the maximum temperature within the effective cutting time. The measured, the calculated, and the predicted cutting temperatures of the workpiece are shown in Fig. 14. As it can be seen, at the beginning, the cutting temperature increases with the increasing feed speed, due to increase in the removed material per unit time. But in

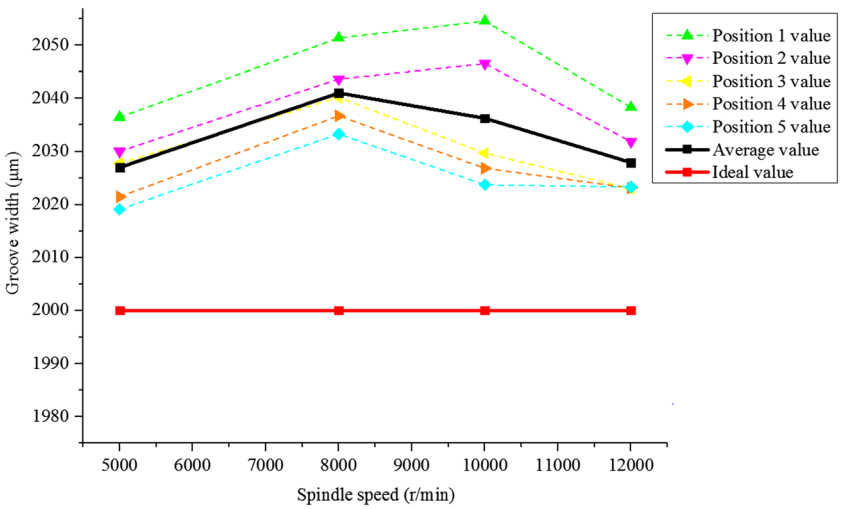

Fig. 17 The influence of spindle speed on the deformation value of the workpiece

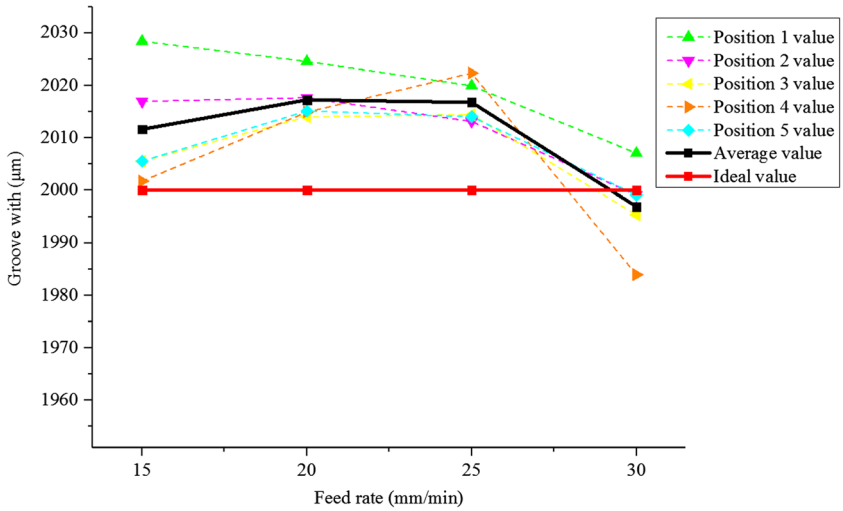

Fig. 18 The influence of feed rate on the deformation value of the workpiece

the end, the cutting temperature decreases with the increasing feed speed, which is because the specific cutting force and the specific cutting power decrease (as shown in Fig. 15), and the cutting time also decreases.

4.3 Analysis of workpiece deformation in micro-milling

In order to study the influencing factors and the variation rules of the workpiece deformation during micro-milling, the deformation value (*D* value of the ideal value and measured value) of the groove side S1 is measured by the Keyence microscope. Firstly, the external side S2 of the workpiece is finished before milling groove in order to ensure the accuracy of the deformation value, and then the whole groove is machined when the workpiece is cooling. Finally, the groove depth is studied by selecting five positions to measure the width (*d*) (as Fig. 16 shows), and taking the mean value as the nominal width of the groove.

In theory, the width is 2000 μm, and the rules of deformation value are shown in Figs. 17 and 18. According to Fig. 17 (the measurements of the test nos. 1 to 4), the deformation range is from 25 to 40 μm; it does not increase or decrease with the increase of spindle speed, but when speed is 8000 r/min, it has a maximum value called "inflection point" in this paper. As shown in Fig. 18 (the measurements of the test nos. 5 to.8), the deformation range is from − 5 to 20 μm,;it does not increase or decrease with the increase of feed rate, but when feed is 25 mm/min, it has a maximum value.

As aforementioned, an "inflection point" can be observed from both the speed and feed experiments, which manifests a significant difference between macro- and micro-milling. It could be explained that the maximum deformation appears as a result of thermo increases but also due to the force increases. Actually, force is indirectly influenced by heat; temperature rise leads to the reduction of friction coefficient and deformation coefficient, thereby reducing the force. When over *M*, the specific cutting force and the specific cutting power decrease, and heat decreases too. The change of the deformation could be illustrated by Fig. 19: when reaching a certain value *L* (spindle speed or feed rate), the effect of force is greater than that of heat, there is an increasing tendency of deformation; above this limit of *L*, heat would play a leading role while deformation still increases; and when increases to *M*, the deformation decreases.

For a single groove, the dimension of the five positions is shown in Fig. 20 (under different spindle speed) and Fig. 21 (under different feed rate). It could be seen from position 1 to position 5 that the size of the groove is gradually reduced. In

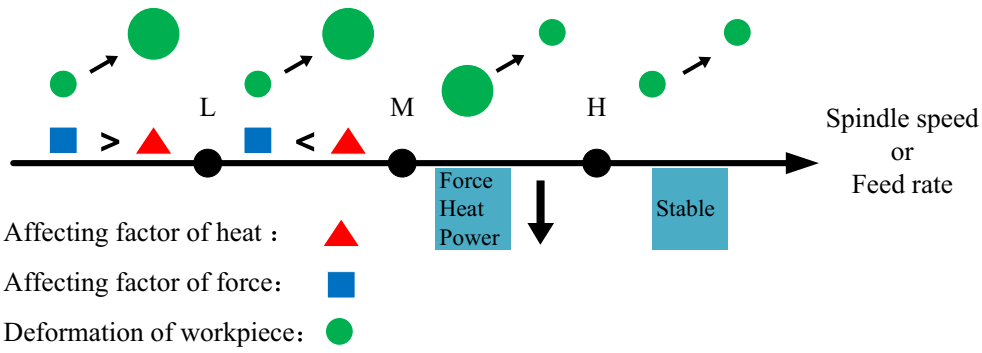

Fig. 19 Deformation with the increase of spindle speed and feed rate

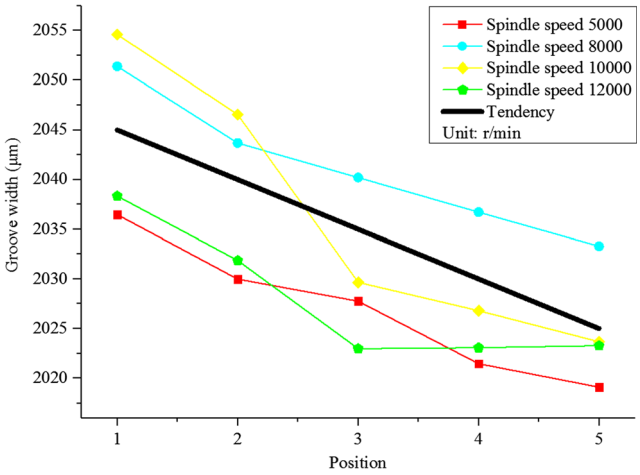

Fig. 20 The deformation value of five positions under different spindle speed

addition, the influence of the spindle speed is greater than that of the feed rate. During the milling process, each groove is machined ten times (with each cutting depth 0.2 mm, the accumulated depth of groove is 2 mm). For each groove, it is machined the most times at position 1, second most at position 2, and least at position 5 In theory, each machining is not affected by the next, but due to the force and heat, more material will be removed during the next machining session. Thus, accounting for size, the upper width of the groove is larger than that of the lower.

5 Conclusions

In this paper, based on the theoretical model of the temperature field, the temperature and the deformation effected by thermo-mechanical coupling are predicted and simulated; then, a series of new design micro-milling experiments are carried out with the purpose of verifying the accuracy of the prediction. In terms of the presented results and discussions above, important conclusions can be drawn as follows:

(1) The calculated, the measured, and the simulated temperatures are in good agreement, which proves the correctness of the theoretical model of temperature rise and the temperature measurement method.
(2) The spindle speed and feed rate have a great influence on the temperature. As the spindle speed increases, the temperature rises disproportionally; as the feed rate increases, the temperature initially increases but ultimately decreases.
(3) The spindle speed and feed rate have a significant impact on the deformation. The deformation does not increase or decrease with the increase of spindle speed or feed rate. However, when the spindle speed is 8000 r/min or feed rate is 25 mm/min, the deformation has a maximum value called “inflection point,” which is caused by thermal-mechanical coupling.
(4) When the rate of material removal is same, higher spindle speed is better for reducing deformation. When the spindle speed is same, higher material removal rate (feed rate) is better for reducing deformation. In order to improve the machining efficiency, selecting high spindle speed and feed rate has a great significance on promoting the workpiece quality in micro-milling.

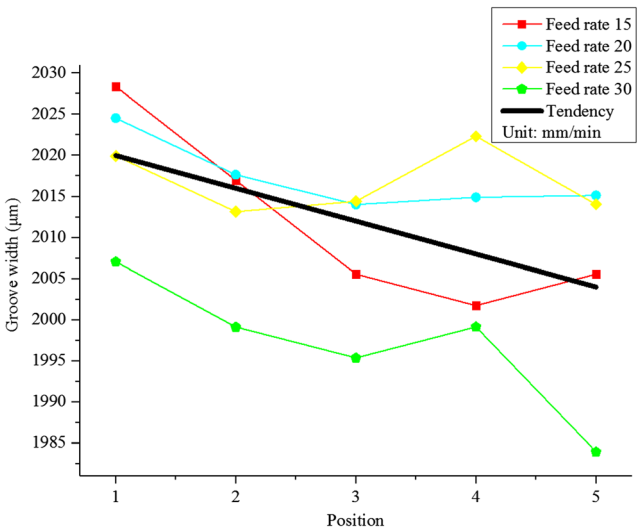

Fig. 21 The deformation value of five positions under different feed rate

Acknowledgements This work has been supported by the Natural Science Foundation of China (No.51575050 and No.51505034).

References

1. Masuzawa T, Tönshoff HK (1997) Three-dimensional micromachining by machine tools. CIRP Ann Manuf Technol 46(2):621–628
2. Liu X, DeVor RE, Kapoor SG, Ehmann KF (2004) The mechanics of machining at the microscale: assessment of the current state of the science. J Manuf Sci Eng 126(4):5064–5070
3. Chae J, Park SS, Freiheit T (2006) Investigation of micro-cutting operations. Int J Mach Tools Manuf 46(3–4):313–332
4. Liu K, Melkote SN (2007) Finite element analysis of the influence of tool edge radius on size effect in orthogonal micro-cutting process. Int J Mech Sci 49(5):650–660
5. Bao WY, Tansel IN (2000) Modeling micro-end-milling operations. Part I: analytical cutting force model. Int J Mach Tools Manuf 40(15):2155–2173
6. Bao WY, Tansel IN (2000) Modeling micro-end-milling operations. Part II: tool run-out. Int J Mach Tools Manuf 40(15):2175–2192
7. Bao WY, Tansel IN (2000) Modeling micro-end-milling operations. Part III: influence of tool wear. Int J Mach Tools Manuf 40(15): 2193–2211

8. Vogler MP, KaPoor SG, Devor RE (2004) On the modeling and analysis of machining performance in micro-end-milling, part11: cutting force prediction. J Manuf Sci Eng 126(4):695–705
9. Zhou Z (1985) Metal cutting principle. Shanghai Scientific and Technical Publishers Shanghai, pp 28–62
10. Push AV (1987) Predication of thermal displacements in spindle units. Sov Eng Res 5(5):42–47
11. Lin S, Peng F, Wen J (2013) An investigation of workpiece temperature variation in end milling considering flank rubbing effect. Int J Mach Tools Manuf 73(7):71–86
12. Grzesik W, Bartoszuk M, Nieslony P (2005) Finite element modelling of temperature distribution in the cutting zone in turning processes with differently coated tools. J Mater Process Technol s164–165(10):1204–1211
13. Jiang F, Liu Z, Wan Y (2013) Analytical modeling and experimental investigation of tool and workpiece temperatures for interrupted cutting 1045 steel by inverse heat conduction method. J Mater Process Technol 213(6):887–894
14. Carvalho SRD, Machado AR, Silva MBD (2014) Analyses of effects of cutting parameters on cutting edge temperature using inverse heat conduction technique. Math Probl Eng (6):1–11
15. Rai JK, Xirouchakis P (2009) FEM-based prediction of workpiece transient temperature distribution and deformations during milling. Int J Adv Manuf Technol 42(5–6):429
16. Lazoglu I, Altintas Y (2002) Prediction of tool and chip temperature in continuous and interrupted machining. Int J Mach Tools Manuf 42(9):1011–1022
17. Yang Y, Zhu W (2014) Study on cutting temperature during milling of titanium alloy based on FEM and experiment. Int J Adv Manuf Technol 73:1511–1521
18. Hsu CY, Huang CK, Wu CY (2007) Milling of MAR-M247 nickel-based superalloy with high temperature and ultrasonic aiding. Int J Adv Manuf Technol 34(9–10):857–866
19. Zhang F (2012) Investigations on transient cutting temperature of tool and workpiece in high-speed milling. Shandong University
20. Luo Z (2009) Thrmo mechanical coupling simulation and experimental study of micro milling process. Harbin Institute of Technology, pp 12–34
21. Tang D, Sun H, Jiao L (2008) A study on prediction approach of the workpiece's face milling deformation. Trans Beijing Inst Technol 28(8):678–681
22. Liu G, Tan G, Li G (2009) Experiment, modeling, and analysis for temperature field of milling insert. Int J Adv Manuf Technol 40(1–2):67–73
23. Richardson DJ, Keavey MA, Dailami F (2006) Modelling of cutting induced workpiece temperatures for dry milling. Int J Mach Tools Manuf 46(10):1139–1145
24. Kaminise AK, Guimarães G, Silva MBD (2014) Development of a tool–work thermocouple calibration system with physical compensation to study the influence of tool-holder material on cutting temperature in machining. Int J Adv Manuf Technol 73(5–8):735–747
25. Chen G, Ren C, Zhang P (2013) Measurement and finite element simulation of micro-cutting temperature of tool tip and workpiece. Int J Mach Tools Manuf 75(12):16–26
26. Rahman M, Kumar AS, Salam M- u (2003) Effect of chilled air on machining performance in end milling. Int J Adv Manuf Technol 21(10–11):787–795
27. Thepsonthi T, Hamdi M, Mitsui K (2009) Investigation into minimal-cutting-fluid application in high-speed milling of hardened steel using carbide mills. Int J Mach Tool Manuf 49(2):156–162
28. Cao Y, Zhang H, Dong H, Li M (2006) Comparison Study on Dry and Wet Cutting Quenched Steel with PCBN. Tool Eng 40(5):19–21
29. Jia G, Wang X (2016) Experimental study on dry and wet cutting of coated carbide tools. Sci Res (12):138–139
30. Hou Z, He S, Li S (1984) Solid heat conduction. Shanghai science and Technology Press, Shanghai
31. Beck JV, Blackwell B, Clair CR (1985) Inverse heat conduction: ill-posed problems. A Wiley-Interscience Publication, Hoboken